

Superconductivity in ternary rare earth
palladium Heusler compounds

by

Martin Joseph Johnson

A Thesis Submitted to the
Graduate Faculty in Partial Fulfillment of the
Requirements for the Degree of
MASTER OF SCIENCE

Department: Physics
Major: Solid State Physics

Signatures have been redacted for privacy

Iowa State University
Ames, Iowa

1984

Superconductivity in ternary rare earth
palladium Heusler compounds

Abstract

A study of the ternary rare earth palladium Heusler compounds of composition RPd_2X , where $R=Sc, Y, Er, Tm, Yb,$ or Lu , and $X=Sn$ or Pb , was undertaken to investigate the behavior of their superconducting transition temperature under pressure. The transition temperature was linearly depressed to 20 kbar, with dT_c/dP typically of the order of 10^{-5} K/bar, which can be explained by a stiffening of the simple cubic palladium sublattice with increasing pressure. The lattice parameter and transition temperature are very disorder-dependent, increasing to maximum values after annealing for two days; resistivity measurements indicate that no phase transitions occur below room temperature.

TABLE OF CONTENTS

	<u>Page</u>
I. INTRODUCTION	1
A. Ternary Superconductors	1
B. Heusler Alloys	3
II. EXPERIMENTAL TECHNIQUES	6
A. Sample Synthesis	6
B. Crystallographic Analysis	6
C. Magnetic Susceptibility Measurements	8
D. Electrical Resistivity Measurements	9
III. EFFECTS OF ANNEALING TIME ON LATTICE PARAMETER AND SUPERCONDUCTING TRANSITION TEMPERATURE	10
A. Introduction	12
B. Results and Discussion	13
IV. PRESSURE DEPENDENCE OF SUPERCONDUCTING TRANSITION TEMPERATURE	18a
A. Introduction	18a
B. Results	18b
C. Discussion	25
V. ELECTRICAL RESISTIVITY MEASUREMENTS	29
A. Introduction	29
B. Results and Discussion	30
VI. ErPd ₂ Sn	36
VII. SUMMARY AND CONCLUSIONS	40

	<u>Page</u>
VIII. REFERENCES	43
IX. ACKNOWLEDGEMENTS	46
X. APPENDIX: SOURCES AND PURITIES OF STARTING MATERIALS	47

I. INTRODUCTION

A. Ternary Superconductors

In the past fifteen years the study of ternary superconductors has grown rapidly.¹ These materials have stimulated the work of experimentalists and theorists alike by exhibiting many new or unusual phenomena such as valence fluctuations and the Kondo effect. Ternary superconductors also have great potential in the field of superconducting technology because of their unique physical properties, such as the very high critical field strengths of some ternary Chevrel phase materials (~ 60 Tesla).

The competition of long range magnetic order and superconductivity is another source of interest in these compounds, because many ternary materials have a regular lattice of magnetic atoms and are nonetheless superconductors. Two types of competitive phenomena have been observed: reentrant superconductivity, where superconductivity is destroyed by the onset of ferromagnetism, and the coexistence of magnetism and superconductivity, where the material simultaneously supports superconductivity and long range oscillatory or antiferromagnetic order. It has been noted² that superconductivity and magnetism occur most commonly in compounds containing the heavy rare earth elements, and that Er is the rare earth element most often involved in coexistence or reentrant phenomena.

The systems investigated in the past share several characteristics. Most ternary superconductors have high crystallographic symmetry, though unlike the best binary superconductors, few are cubic. With the exception of $\text{Ba}(\text{Pb},\text{Bi})\text{O}_3$, all contain transition metals as major constituents. Frequently, the interplay of magnetism and superconductivity is present. Because they are composed of three elements, all of which are on unique crystallographic sites, there is a much greater choice of compositions as compared to binary materials. The systems studied often allow a wide variety of atomic species to be substituted on the third element sites. However, these last two factors may be due to the choice of systems studied rather than an inherent property of ternary superconductors.

In 1971, R. Chevrel et al.³ characterized the ternary molybdenum chalcogenides MMo_6S_8 and MMo_6Se_8 , the so-called Chevrel phase materials. These molybdenum cluster compounds include the reentrant superconductor HoMo_6S_8 . The ternary rare earth borides, first reported superconducting by B. T. Matthias et al.⁴ and D. C. Johnston⁵ in 1977, are also cluster compounds, crystallizing in the CeCo_4B_4 -type and LuRu_4B_4 -type structures, respectively. Since then, superconducting borides with 1:3:2 and 1:1:2 composition ratios (rare earth: transition metal:boron) have also been discovered.^{6,7,8} The ternary silicides, germanides, and stannides reported by

H. F. Braun,⁹ C. V. Segre and Braun,¹⁰ and J. P. Remeika et al.,¹¹ since 1980 include $Tm_2Fe_3Si_5$, a reentrant superconductor.

B. Heusler Alloys

In this study, some superconducting Heusler alloys are investigated by means of ac susceptibility measured at high pressure and electrical resistivity experiments. The term Heusler alloy refers to a class of atomically well-ordered intermetallic ternary compounds having the general composition of XY_2Z . The constituent atoms occupy crystallographically non-equivalent positions in a cubic $L2_1$ structure (space group $Fm\bar{3}m$). The Y atoms form a simple cubic sublattice, with the X and Z atoms forming a NaCl-type sublattice occupying the body-center positions of the first sublattice.

The Heusler alloys have been widely investigated because of their magnetic characteristics.¹² In 1903, F. Heusler reported that the $MnCu_2Z$ -type compounds, where the third element was from the IIIB, IVB, or VB columns of the periodic table, were ferromagnetic.¹³ This was surprising because the constituents were diamagnetic or paramagnetic, at a time when all known ferromagnets contained ferromagnetic components. Substitution of transition metals such as Ni, Co, Pd, and Rh for the X component (Cu) also yields ferromagnetic materials. Many Heusler alloys are now known.¹⁴ Interestingly, the Heusler alloy $MnPd_2Sn$, with the Mn atoms replacing the rare

earth atoms of this investigation, orders ferromagnetically at 189 K.¹⁵

In this work, we focus on some ternary rare earth palladium Heusler compounds. These materials were first investigated by Ishikawa et al.,¹⁶ and are the first reported Heusler superconductors. In these materials, the rare earth and tin (or lead, in YPd_2Pb) atoms form the NaCl-type sublattice on the body-centered positions of a palladium simple cubic sublattice (see Figure 1). From specific heat and upper critical field measurements, Ishikawa et al. suggested that superconductivity was due to the palladium d-electrons. The rare earths from Gd to Lu, as well as Sc and Y, can be inserted in the lattice; since the Tm, Yb, and possibly the Er samples are superconducting, these materials represent a new family of magnetic superconductors. Both high and low temperature resistivity data and the effects of pressure on the superconducting transition temperature are reported in this thesis for some Heusler superconductors. A study of the effects of annealing time on lattice parameter and superconducting transition temperature and some preliminary data on the possible interplay of magnetism and superconductivity in $ErPd_2Sn$ are also presented.

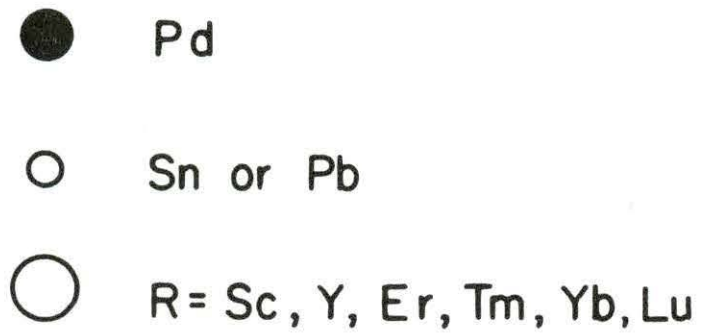
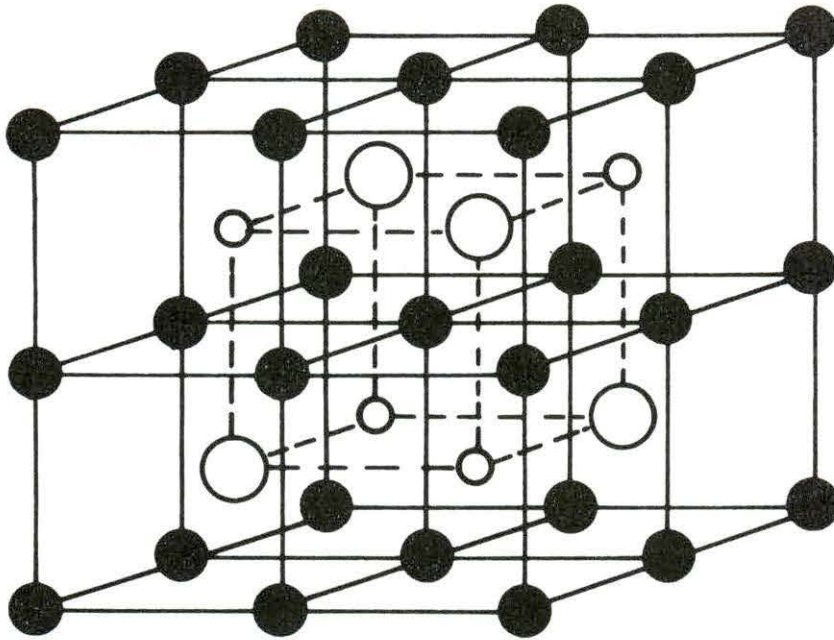


Figure 1. Structure of the Heusler superconductors

II. EXPERIMENTAL TECHNIQUES

A. Sample Synthesis

Starting materials for all samples were high purity elements, with sources and purities listed in the Appendix. Lead rod used in the synthesis of YPd_2Pb was etched in 1:1 mixture of acetic acid and hydrogen peroxide to remove surface impurities. The materials were arc-melted on a water-cooled copper hearth in a Zr-gettered argon atmosphere. In the case of the Yb and Tm samples, there was considerable mass loss during arc-melting due to the high vapor pressures of Yb and Tm relative to the other constituents. Additional Yb and Tm were added to bring the sample mass up to its pre-melting value. Palladium and tin powders were individually arc-melted to spheres before weighing to prevent loss of the powders within the furnace and to drive off impurities. To assure homogeneity in the samples, most were then sealed in quartz tubes under a partial pressure of argon and then annealed for several days at 900 to 1000°C. Mass loss during annealing was negligible in all samples. Details of sample preparation are presented in Table 1.

B. Crystallographic Analysis

Pieces of the samples were easily ground in an agate mortar to powders, since the materials were quite brittle. Powder x-ray diffraction data were obtained for each sample using a microcomputer-controlled Rigaku powder diffractometer

Table 1. Details of sample preparation

sample number	compound	heat ^a treatment	lattice parameter (Å)	comments ^b
1-23	ScPd ₂ Sn	2d 1000	6.509 ± .062	P,R,T
1-10	YPd ₂ Sn	none	6.716 ± .011	some impurities
1-11	YPd ₂ Sn	3d 900	6.719 ± .039	P,R,T
1-14	YPd ₂ Pb	2d 900	6.778 ± .011	some impurities
1-16	YPd ₂ Pb	2d 900	6.786 ± .008	P,R,T
1-19	ErPd ₂ Sn	none	6.684 ± .015	P,R,T
1-13	TmPd ₂ Sn	3d 900	6.653 ± .001	many impurities
1-15	TmPd ₂ Sn	2d 900	6.668 ± .003	P,T
1-17	TmPd ₂ Sn	none	6.668 ± .007	many impurities
1-24	TmPd ₂ Sn	2d 1000	6.670 ± .024	many impurities
1-26	TmPd ₂ Sn	2d 1000	6.670 ± .005	R
1-12	YbPd ₂ Sn	3d 900	6.657 ± .007	P,T
1-25	YbPd ₂ Sn	2d 1000	6.653 ± .014	R
1-18	LuPd ₂ Sn	see Chapter III		A,P,R,T
1-22	LuPd ₂ Sn	see Chapter III		A

^a2d 1000 denotes 2 days at 1000°C.

^bA denotes use in annealing study
P denotes use in pressure study
R denotes use in resistivity study
T denotes use in transition temperature study.

equipped with copper target and graphite monochromator for Cu K α radiation. A scan rate of 0.6 degrees per minute and a step width of 0.01 degrees per step were used over the 2θ angular range of 20 to 140 degrees. The angular positions of peaks were determined from the raw data using a 16 point smoothing function and were defined as the midpoint of full peak width taken at half maximum peak intensity. A standard least squares fitting routine¹⁷ was used to determine the lattice parameter from the peak positions. In most cases, the accuracy of the lattice parameters determined by this method was better than 0.1%.

The program LAZY PULVERIX¹⁸ was used to calculate a powder diffraction pattern given the crystallographic space group, the positions of the atoms in the unit cell, and an estimated value of the lattice parameter. The output of LAZY PULVERIX consists of the calculated peak positions and their intensities, which were then compared to the measured pattern. For most samples, there was excellent agreement between the measured and calculated peak positions and intensities, with no impurity peaks observed.

C. Magnetic Susceptibility Measurements

The ambient pressure superconducting transition temperature (T_c) of the samples was determined from low frequency (~ 25 Hz) ac magnetic susceptibility measurements in a conventional dewar for the 1.2-25 K temperature range. In addition,

measurements of magnetic susceptibility for a sample of ErPd_2Sn were performed using a S.H.E. Corporation helium dilution refrigerator for the 0.060-11 K temperature range. In all cases, the midpoint of the transition was taken as T_c , and 10% and 90% points were used to define the transition width.

The change in superconducting transition temperature as a function of pressure was determined to approximately 20 kbar (2 GPa) for bulk pieces of the samples using a hardened beryllium copper hydrostatic pressure clamp with tungsten carbide pistons.¹⁹ A measurement of the ambient pressure transition temperature was made at the end of each series of pressure measurements; in all cases the agreement with the original measurement was good, indicating complete reversibility of the pressure effects on T_c . A 1:1 mixture of isoamyl alcohol and n-pentane was used in the pressure transmitting fluid, and pressures were determined at low temperatures using superconducting lead and tin manometers.²⁰ The value of dT_c/dP was calculated using a least squares fitting routine.

D. Electrical Resistivity Measurements

The ac electrical resistivity of each sample was measured using the four probe technique. Pieces used were slices of ingots with thicknesses of approximately 1 mm and round or oval shapes with diameters of approximately 3 to 5 mm. Four 0.002 inch diameter platinum wires were equidistantly affixed

to the perimeter of a sample face using silver epoxy, and then soldered to four posts on the sample holder. A small alternating current, typically 20 mA peak to peak, was sent through two adjacent wires, and the voltage across the other pair was measured using a Princeton Applied Research (PAR) Model 124A lock-in amplifier. For the YPd_2Sn and LuPd_2Sn samples, the sample voltage was amplified using a PAR Model 116 differential pre-amplifier to increase the sample voltage by a factor of 100 before going to the lock-in amplifier. The current was determined by measuring the voltage across a standard $1\text{ m}\Omega$ resistor with the lock-in amplifier. By admitting a small amount (about 10 mtorr) of helium exchange gas to the vacuum can surrounding the sample holder, the temperature of the sample was allowed to decrease slowly (approximately 100 K/hour) to that of the surrounding bath, and measurements were taken from room temperature to just below the superconducting transition; measurements below 4.2 K were made while pumping on the helium bath. A calibrated platinum thermometer was used in the 30-300 K temperature range, and a calibrated carbon glass thermometer was used below 30 K.

The method of L. J. van der Pauw²¹ was used to determine the specific resistivity values from the measured voltages; the use of this method is outlined in Chapter V. The sample thickness used in calculations was measured with vernier calipers. Because the sample current was essentially constant

over the entire temperature range, the value of $\rho(T)/\rho(300\text{ K})$ was the sample voltage at temperature T divided by the sample voltage at room temperature. Resistivity values have uncertainties, due mainly to the scatter in voltage values, of approximately $\pm 5\ \mu\Omega\text{-cm}$.

III. EFFECTS OF ANNEALING TIME ON LATTICE PARAMETER AND SUPERCONDUCTING TRANSITION TEMPERATURE

A. Introduction

As past studies have shown, crystallographic order has a profound effect on superconductivity. Cox et al.²² irradiated high T_c (~ 20 K) Al5 binary compounds like Nb_3Ge to produce defects. This effect reduced T_c to less than 2 K while increasing the lattice parameter by 0.03 Å. Cox et al. suggested that the behavior was due to site-exchange disorder, static displacements, or regions of high disorder in an ordered matrix. Disorder in the Al5 system was also studied by M. Lehman et al.,²³ who suggested that from calculations of the electron-phonon coupling constant that T_c was depressed by smearing the fine structure in the electronic density of states at the Fermi level.

The complex crystallographic structure of many ternary superconductors, which seems essential to some of their properties, makes them important systems in which to study the effects of disorder on superconductivity. Irradiation effects in the ternary 1:4:4 rare earth rhodium borides were studied by Dynes et al.,²⁴ who saw an increase in resistivity with the decrease in T_c . Adrian et al.²⁵ suggested that irradiation-produced defects caused a sharp reduction in $N(E_F)$ in the Chevrel phase $Ag_xMo_6S_8$. An investigation into the effects of disorder in Heusler ternary superconductors is reported here.

B. Results and Discussion

Ishikawa et al.¹⁶ report lattice parameter values that agree well with those reported here, but there are large differences in superconducting transition temperatures between the two investigations (see Table 2). Ishikawa et al. also reported that changes in tin concentration of a few atomic percent in samples caused a change in the superconducting transition temperature of 200%, but a change of only 0.3% in the lattice parameter. This sensitivity suggests that disorder is an important factor in determining sample transition temperatures in the Heusler superconductors, as is seen in other ternary systems.

Table 2. Comparison of previous work on superconducting Heusler compounds and present investigation

compound	Ishikawa et al. ¹⁶		this work	
	lattice parameter (Å)	T _c (K)	lattice parameter (Å)	T _c ^a (K)
YPd ₂ Sn	6.702	3.72	6.719 ± .039	5.02 - 4.81
YPd ₂ Pb	6.790	4.76	6.786 ± .008	4.13 - 4.01
ErPd ₂ Sn	6.68	-- ^b	6.684 ± .015	-- ^b
TmPd ₂ Sn	6.67	2.7	6.668 ± .003	1.92 - 1.52
YbPd ₂ Sn	6.65	1.5	6.657 ± .007	1.82 - 1.76
LuPd ₂ Sn	6.64	3.0	6.644 ± .004	2.15 - 3.08

^aT_c¹⁰ - T_c⁹⁰ measured from ingot piece.

^bSee Chapter VI.

As Ishikawa et al noted, the apparent linear behavior of the lattice parameter for the ErPd_2Sn to LuPd_2Sn indicates the rare earth atoms are trivalent in these materials. This can be seen in our measured values of the lattice parameter a (Figure 2). The lattice parameter increases almost $70 \text{ m}\text{\AA}$ upon substitution of lead for tin in YPd_2Sn , though as will be seen in Chapter IV, there is little change in its superconducting properties.

Measurement of lattice parameter and T_c of sample 1-18 of LuPd_2Sn revealed that annealing at 900°C for two days caused an increase in lattice parameter of $4 \text{ m}\text{\AA}$ and an increase in T_c of 0.2 K . A large piece of LuPd_2Sn was synthesized by arc-melting, and sliced into six smaller pieces which were then annealed at 1000°C for up to 14 days. The pieces were then ground to powders, and the lattice parameter and T_c were measured. Table 3 contains a summary of the annealing time, lattice parameter, and T_c for these samples.

Annealing increased the lattice parameter by about $4 \text{ m}\text{\AA}$ and T_c by 0.2 K consistently in LuPd_2Sn , with the lattice parameter and T_c reaching a maximum after two days annealing at 1000°C . Further annealing caused no further increase in transition temperatures. X-ray diffraction patterns of the samples had no observed impurity peaks, indicating that impurity phases made up less than 5% of the samples. There were no appreciable changes in the diffraction pattern line

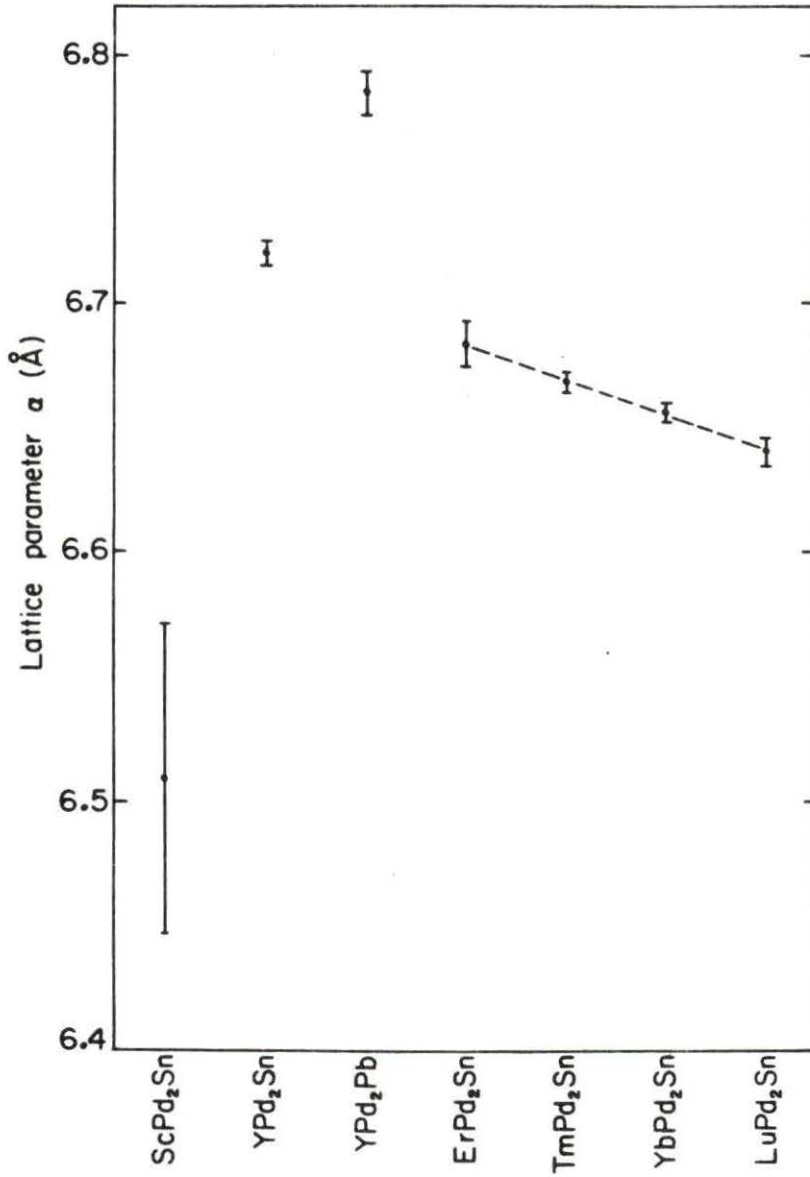


Figure 2. Lattice parameter a of some Heusler superconductors

Table 3. Effects of heat treatment on lattice parameter and critical temperature in LuPd₂Sn

sample number	heat ^a treatment	lattice parameter (Å)	T _c ^b (K)
1-18a	none	6.6405 ± .0087	2.89 - 2.84 - 2.69
1-18a	2d 900	6.6440 ± .0076	3.14 - 3.09 - 2.89
1-22a	none	6.6406 ± .0037	2.88 - 2.79 - 2.64
1-22b	2d 1000	6.6438 ± .0073	3.03 - 2.98 - 2.83
1-22c	4d 1000	6.6441 ± .0049	3.02 - 2.99 - 2.82
1-22d	6d 1000	6.6439 ± .0077	3.03 - 2.98 - 2.77
1-22e	14d 1000	6.6441 ± .0034	3.02 - 2.98 - 2.79
1-22f	14d 1000 W	6.4442 ± .0046	3.01 - 2.98 - 2.75

^a2d 1000 denotes 2 days at 1000°C.

^bT_c¹⁰ - T_c⁵⁰ - T_c⁹⁰.

W denotes water quenching.

widths with annealing, indicating that the lattice parameter was quite uniform throughout the samples, before and after annealing. Sample 1-22f was cooled quickly by water quenching, but it did not differ significantly in lattice parameter or T_c from sample 1-22e, which was annealed for the same time but allowed to slowly air cool (probably several orders of magnitude more slowly than water quenching).

The lattice parameter is relatively insensitive to sample synthesis, but T_c varies from sample to sample, as can be seen in Tables 2 and 3. The increase in lattice parameter might be attributed to the larger lutetium atoms ordering themselves into the simple cubic palladium sublattice; the stability of the line widths indicate that there is no large scale inhomogeneities in the samples. Ishikawa et al. note that large changes in T_c due to ordering are characteristic of materials having sharp structure in the density of states such as the Al5 compounds. Eiling et al.²⁶ suggest that rare earth vacancies cause potential fluctuations and thus a broadening of the density of states curve in the lanthanum chalcogenides. In the future, the density of states as a function of pressure of these materials should be calculated to compare these models, as well as to support a quantitative study of disorder in these materials.

IV. PRESSURE DEPENDENCE OF SUPERCONDUCTING TRANSITION TEMPERATURE

A. Introduction

The decrease in superconducting transition temperature seen in most s- and p-metals has been described in a simple lattice model.²⁷ Pressure causes the lattice to stiffen and shifts the phonon spectrum to higher energies. This process weakens the electron-phonon interaction and causes a decrease in T_C .

The simple lattice model fails to explain the often complex behavior of T_C under pressure in transition metal superconductors. The many positive and negative pressure effects are attributed to electronic effects.²⁸ Structural transformations, Fermi surface topology, and competitive phenomena have been suggested to explain non-linear pressure effects observed in elements such as La and U, and in many compounds.

The behavior of T_C under pressure in the Chevrel phases and ternary iron silicides are illustrative of the unusual behavior often seen in ternary superconductors. In the Chevrel phase system $Cu_xMo_6S_8$, T_C increases from 10.5 K to 11.7 K at 6 kbar, then decreases under higher pressures,²⁹ while in $ScMo_6S_8$, T_C continues to increase for pressures above 20 kbar. Segre and Braun³⁰ report that T_C in $Y_2Fe_3Si_5$ increases from 2.2 to 4.8 K at 13 kbar, a pressure effect that is an order of magnitude larger than that normally observed.

Vining and Shelton³¹ have noted that for many of the Chevrel materials and the ternary iron silicides, T_c appears to be linearly related to dT_c/dP . It is believed that this is caused by changes in Fermi surface topology with pressure.³² This may be confirmed by calculations of the band structures of these materials.

In this investigation the pressure dependence of T_c in the Heusler superconductors is studied to 20 kbar. Since the Heusler superconductors represent a new family of ternary superconductors, this study will add additional information to that already collected on the effects of pressure on T_c in the Chevrel phase, rhodium boride, and iron silicide systems.

B. Results

In Figure 3 the superconducting transition temperatures are plotted as a function of pressure. In all cases, T_c is depressed by increasing pressure to the highest pressures attained (about 20 kbar), with the depression rate on the order of 10^{-5} K/bar. For most samples, the error bars indicate the 10% and 90% points of the transition. The $TmPd_2Sn$ sample had an especially broad transition which extended below the minimum attainable temperature of the apparatus at pressures above about 18 kbar; since the transition shape was constant with pressure, a feature near the transition midpoint was used to define the transition temperature for this sample.

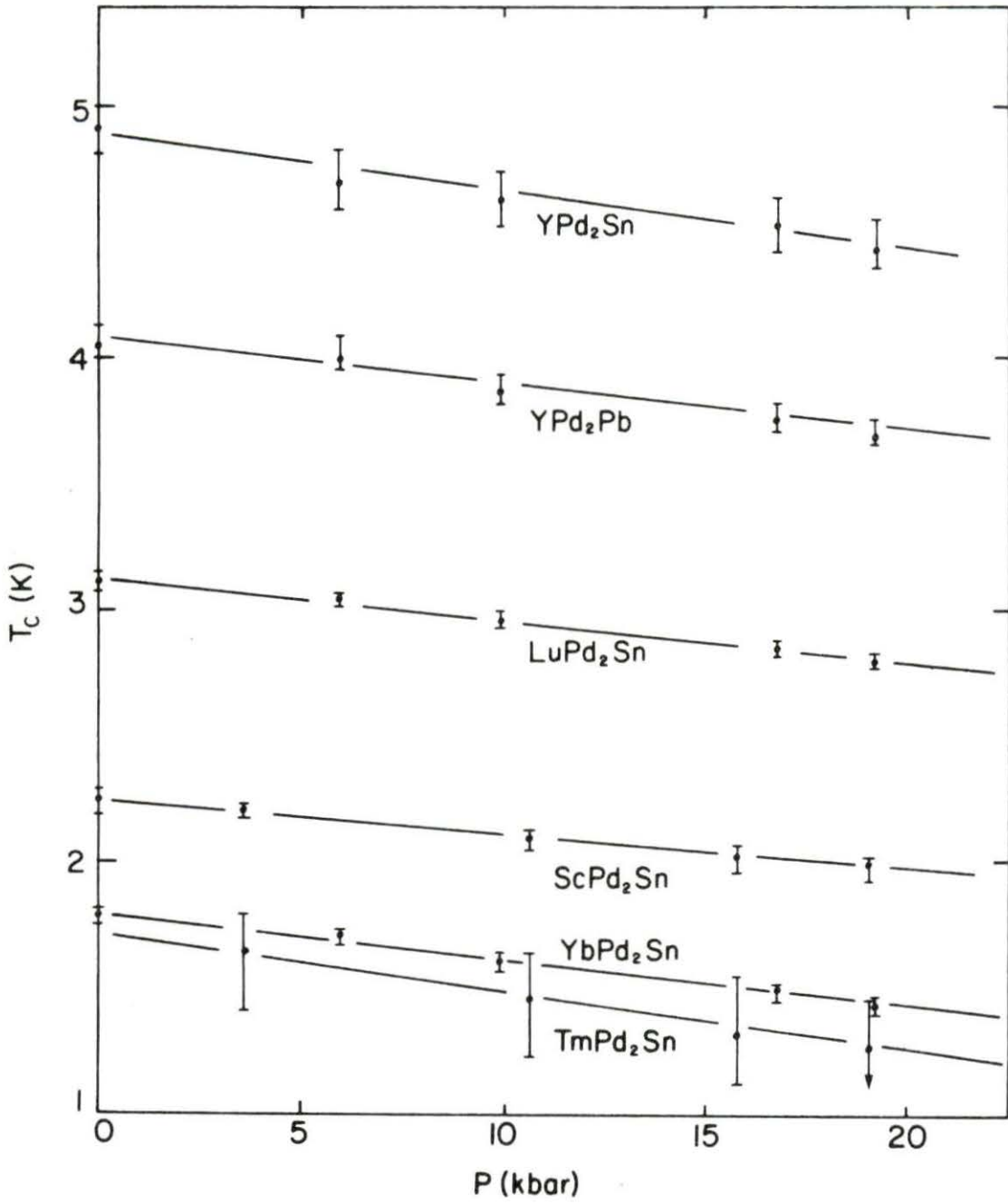


Figure 3. Pressure dependence of superconducting transition temperature (lines are drawn as guides to the eye)

The slope and intercept of the lines best fitting the pressure data were calculated using a least squares fitting routine. The values of dT_c/dP , $d\ln T_c/dP$ and their uncertainties are presented in Table 4; in Figure 4, $-d\ln T_c/dP$ is plotted for these materials, and for samples of tin and lead for comparison.

Table 4. Pressure characteristics of Heusler superconductors

compound	lattice parameter (Å)	T_c^a (K)	$-dT_c/dP$ (10^{-5} K/bar)	$-d\ln T_c/dP$ (10^{-6} /bar)	θ_D^a
ScPd ₂ Sn	6.509 ± .062	2.25	1.448 ± .100	6.44 ± .44	232
YPd ₂ Sn	6.719 ± .039	4.92	2.261 ± .207	4.61 ± .43	165 ^b
YPd ₂ Pb	6.786 ± .008	4.05	1.946 ± .147	4.81 ± .36	198 ^b
TmPd ₂ Sn	6.668 ± .003	1.77	2.620 ± .093	14.80 ± .54	120
YbPd ₂ Sn	6.657 ± .007	1.79	1.933 ± .087	10.92 ± .49	118
LuPd ₂ Sn	6.644 ± .004	3.11	1.684 ± .069	5.43 ± .22	118

^aAt ambient pressure.

^bDetermined from specific heat measurements by Ishikawa et al.¹⁶

The data were analyzed using the method of Eiling et al., who applied it to the lanthanum chalcogenides,²⁶ and we use the framework first applied by McMillan.³³

The superconducting transition temperature is given by the McMillan equation

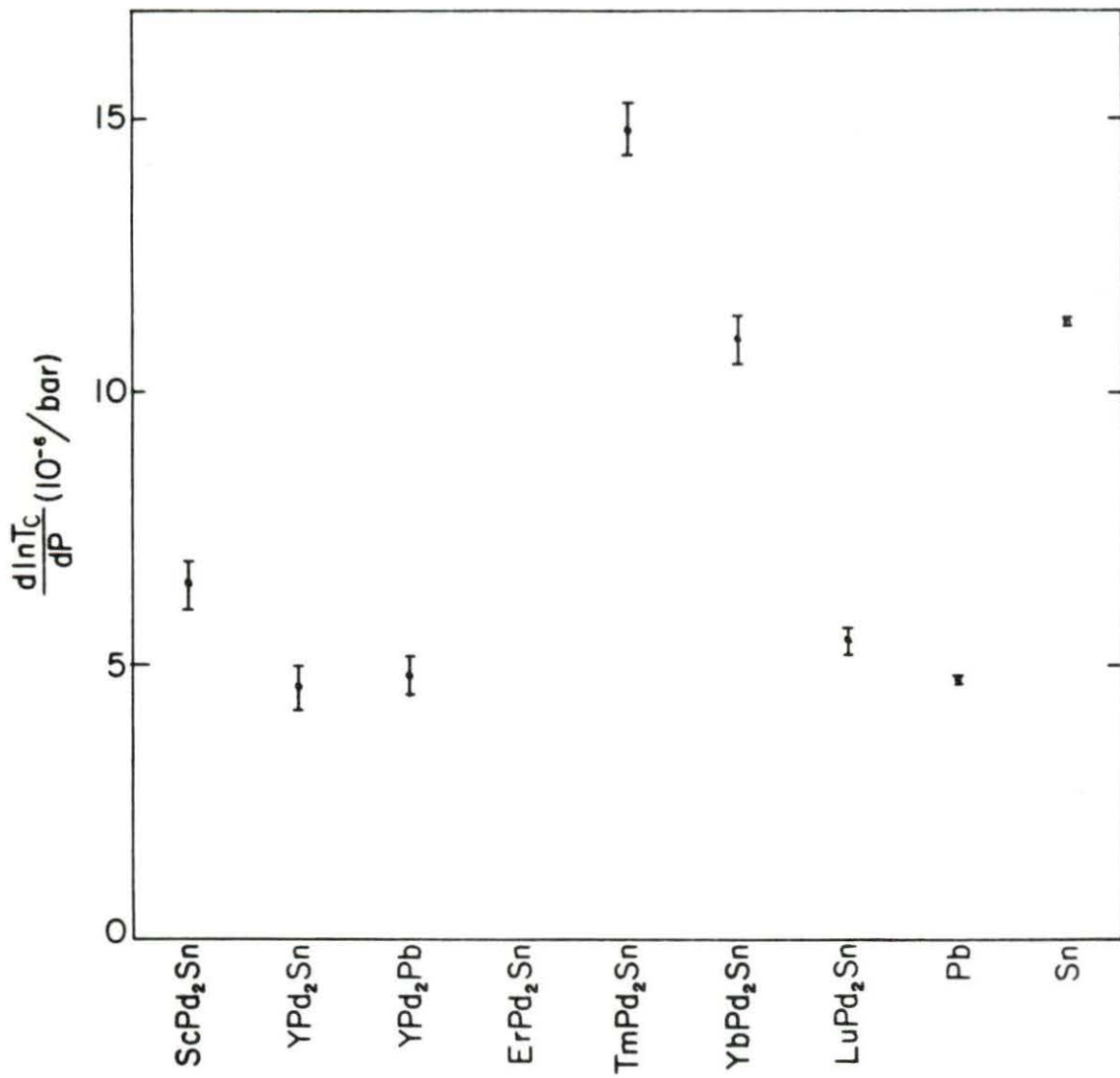


Figure 4. $d \ln T_c / dP$ values of Heusler superconductors (Pb and Sn added for comparison)

$$T_C = \frac{\theta_D}{1.45} \exp \left(- \frac{1.04(1+\lambda)}{\lambda - \mu^*(1+0.62\lambda)} \right), \quad (1)$$

where θ_D is the Debye temperature and μ^* is the effective electron-electron interaction. The electron-phonon coupling constant λ is given by

$$\lambda = \frac{N(E_F) \langle I^2 \rangle}{M \langle \omega^2 \rangle} = \frac{\eta}{M \langle \omega^2 \rangle}. \quad (2)$$

$N(E_F)$ is the density of states at the Fermi level, $\langle I^2 \rangle$ is the average of the squared electron-phonon matrix element, M is the ionic mass, and η is the McMillan-Hopfield parameter, which is described below. The term $\langle \omega^2 \rangle$ is an averaged phonon frequency, which is often approximated by³⁴

$$\langle \omega^2 \rangle = (0.8 \theta_D)^2. \quad (3)$$

Ishikawa et al.¹⁶ determined the Debye temperatures of YPd_2Sn and YPd_2Pb by heat capacity measurements.¹⁶ Estimates of the Debye temperatures for the compounds RPd_2Sn , where $R=Sc, Tm, Yb, \text{ or } Lu$, were made by scaling the measured value for YPd_2Sn ($\theta_D^Y = 165 \text{ K}$) by the rare earth atomic masses using the expression

$$\theta_D^R = \theta_D^Y \left(\frac{M_Y}{M_R} \right)^{1/2}. \quad (4)$$

The Debye temperature values are given in Table 4.

The quantity η in equation (1) is the McMillan-Hopfield parameter, which is a purely electronic parameter, while $M\langle\omega^2\rangle$ is mainly due to the phonons. Since high- T_c superconductors are technologically desirable, factors which increase T_c are interesting. Equation (1) suggests an increase in T_c is possible if λ is increased: this will occur if $N(E_F)$ or $\langle I^2 \rangle$ increase, or if $\langle\omega^2\rangle$ decreases.

The pressure dependence of $\langle\omega^2\rangle$ can be approximated by using the expression of Barron et al.³⁵

$$d\ln\langle\omega^2\rangle/d\ln V = -2\gamma_{Gr} , \quad (5)$$

where γ_{Gr} is the high temperature Gruneisen parameter.

Expression (5) can be rewritten as

$$\frac{d\ln(1/\langle\omega^2\rangle)}{dP} = -\frac{2\gamma_{Gr}}{B} , \quad (6)$$

where B , the bulk modulus, is given by $B = -dP/d\ln V$, and because $\ln\langle\omega^2\rangle = -\ln(1/\langle\omega^2\rangle)$. This conversion facilitates the comparison of changes under pressure in λ and $\langle\omega^2\rangle$ on η using expression (2); also, pressure, rather than volume, is an experimentally adjustable quantity. Solutions of this equation yields

$$\frac{1}{\langle\omega^2\rangle} = \frac{1}{\langle\omega_o^2\rangle} \exp \left(-\frac{2\gamma_{Gr}}{B} P \right) , \quad (7)$$

where $\langle\omega_o^2\rangle$ is $\langle\omega^2\rangle$ at ambient pressure.

An estimated bulk modulus B of 1.25 Mbar (125 GPa) was used for all the compounds since no published measurements of the bulk moduli of Heusler compounds exist. This value was justified by estimates calculated by using a weighted average of the bulk moduli of the constituent elements (ranging from 1.073 Mbar for YbPd_2Sn to 1.181 Mbar for ScPd_2Sn) and by self-consistent local density functional calculations by Kübler³⁶ of the bulk modulus of ScPd , a compound having the simpler CsCl structure, with a bulk modulus of 1.37 Mbar.

Using a bulk modulus of 1.25 Mbar, a pressure of 20 kbar, and a typical transition metal value for γ_{Gr} of 2 ± 0.5 , the value of the exponent is on the order of 1/15. The exponential function can then be expanded, retaining only the first two terms; expression (7) can be rewritten as

$$\frac{1}{\langle \omega^2 \rangle} = \frac{1}{\langle \omega_0^2 \rangle} \left(1 - \frac{2\gamma_{\text{Gr}}}{B} P \right) . \quad (8)$$

Thus, for the pressure achieved in this investigation, $1/\langle \omega^2 \rangle$ is linear with pressure, as is shown in Figure 5.

The values of λ were calculated using the scaled Debye temperatures, the measured transition temperatures, and a typical transition metal value of 0.10 for μ^* , and are shown in Figure 5. The McMillan-Hopfield parameter η is calculated using the equation

$$\eta = \frac{M\lambda}{1/\langle \omega^2 \rangle} . \quad (9)$$

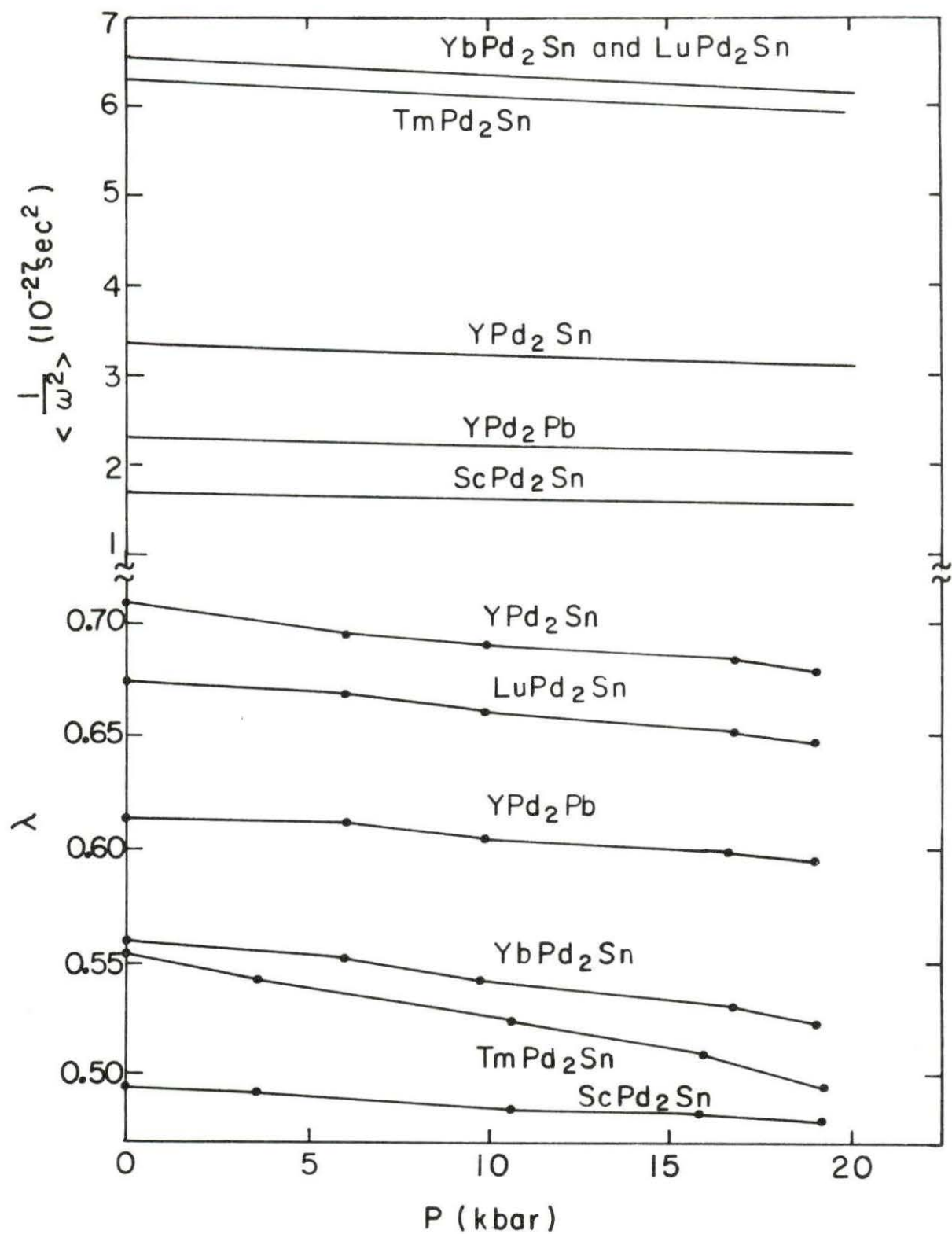


Figure 5. Pressure dependence of λ and $1/\langle \omega^2 \rangle$

The McMillan-Hopfield parameters as a function of pressure for some Heusler superconductors are shown in Figure 6.

C. Discussion

The decrease of T_c with pressure in the Heusler superconductors is comparable in size to the effects seen in the elements and binary compounds, and with none of the exotic behavior seen in other ternary superconducting systems up to 20 kbar. The pressure dependence (Figure 3) appears to be linear to the highest pressures achieved, with a slope varying from -1.448×10^{-5} K/bar for ScPd_2Sn to -2.620×10^{-5} K/bar for TmPd_2Sn . The insensitivity of $d\ln T_c/dP$ to substitution of the non-magnetic rare earths or tin (by lead) suggests that the pressure behavior is determined by its effect on the palladium sublattice (see Figure 4).

The Heusler superconductors show a weak increase in the average squared phonon frequency with pressure as seen in the decrease of $1/\langle \omega^2 \rangle$ with pressure in Figure 5. However, increasing pressure slightly suppresses the electron-phonon interaction, as seen as a decrease in λ . For comparison, lead has a $d\ln T_c/dP$ value of -4.6×10^{-6} /bar, close to that of ScPd_2Sn , YPd_2Pb , and LuPd_2Sn ; TmPd_2Sn and YbPd_2Sn have a $d\ln T_c/dP$ much like that of tin, which has a $d\ln T_c/dP$ value of -11.2×10^{-6} /bar.

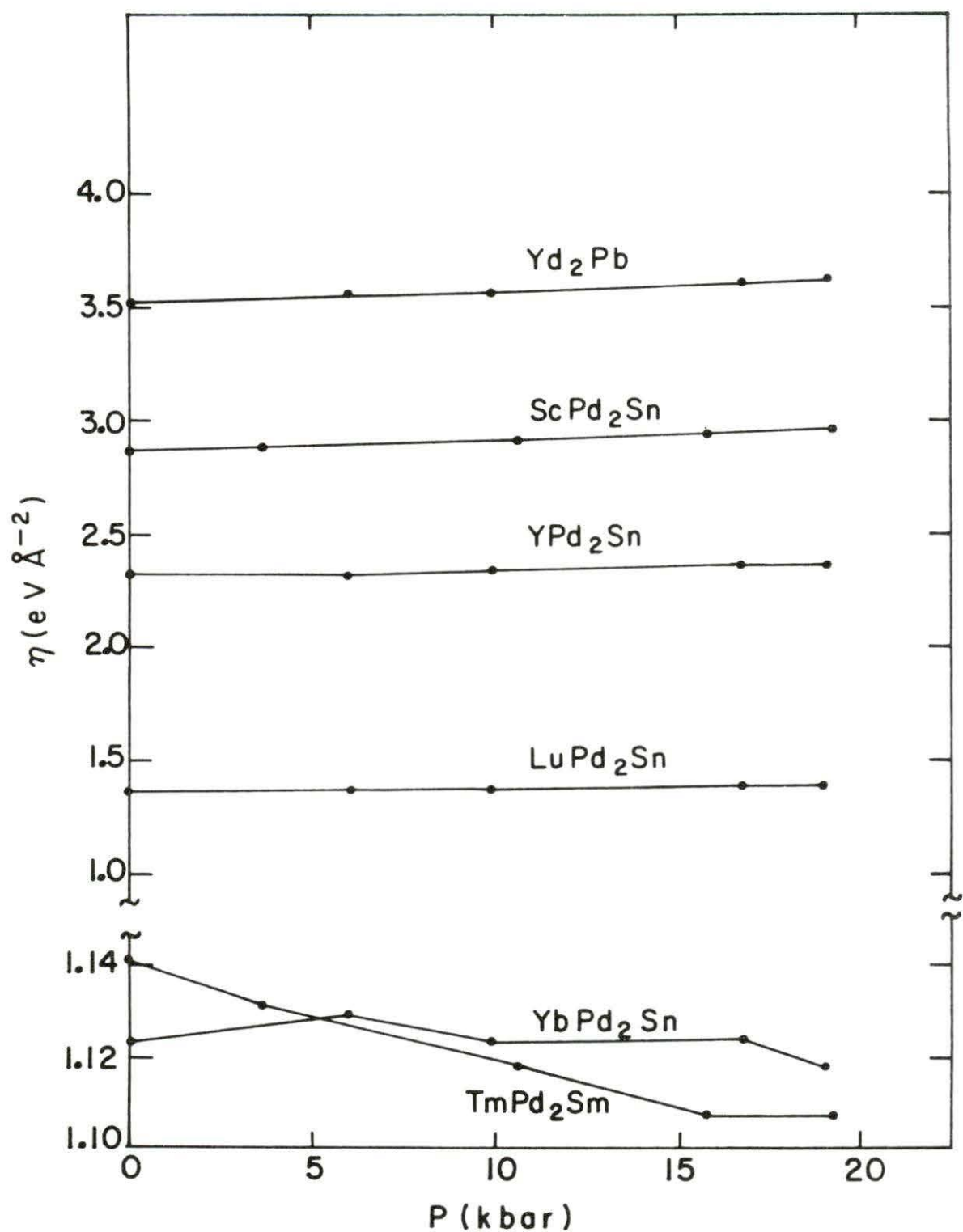


Figure 6. Pressure dependence of η

For all the compounds, the flat slope of the McMillan-Hopfield parameter η with pressure (Figure 6) suggests that the pressure dependence of T_c is mainly due to lattice stiffening. YPd_2Pb , $ScPd_2Sn$, YPd_2Sn , and $LuPd_2Sn$ have a small positive slope which might indicate small increases in the density of states with increasing pressures. However, there does not seem to be the sharp structure in the density of states suggested by Ishikawa et al. from the sensitivity of T_c to tin concentration.

In Figure 7, $-dT_c/dP$ is plotted versus T_c . The plot suggests that there is a linear relationship between dT_c/dP and T_c for some of the Heusler superconductors. This behavior has also been seen in the Chevrel-phase and iron silicide systems, and has been suggested as an indicator of changes in Fermi surface topology with pressure. Vining and Shelton have noted that this behavior seems to be a universal first approximation in ternary systems. The materials containing the magnetic Tm and Yb atoms, however, fall far from the line. It is believed that their magnetic character suppresses T_c enough to remove them from the line. In the future, band structure calculations would help resolve these uncertainties.

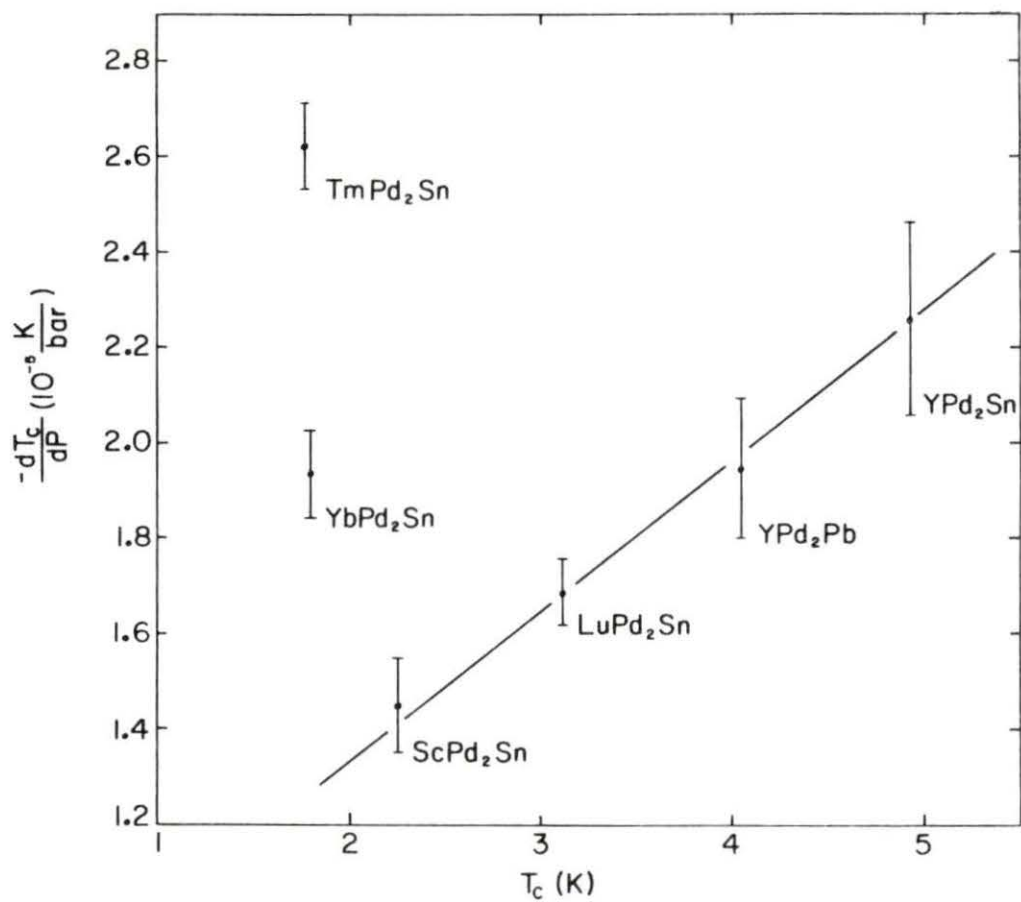


Figure 7. $-\frac{dT_c}{dP}$ versus T_c for some Heusler superconductors (line is drawn as a guide for the eye)

V. ELECTRICAL RESISTIVITY MEASUREMENTS

A. Introduction

The electrical resistivity ρ of a metal in general decreases with temperature in a uniform manner. Resistivity for a metal may be defined by

$$\rho = \frac{m^*}{Ne^2} \frac{1}{\tau} . \quad (10)$$

where m^* is the effective mass of an electron in the material, N is the concentration of conduction electrons, e is the electronic charge, and τ is the scattering time, or time between scattering events. The resistivity is thus proportional to the probability that an electron will scatter per unit time.

There are two causes for electron scattering events:

(1) lattice vibrations (phonons), and (2) lattice imperfections and impurities. The resistivity can be divided into two parts, one for each cause of electron scattering:

$$\rho = \rho_{ph} + \rho_i , \quad (11)$$

where ρ_{ph} is the resistivity contributed by the phonons, and ρ_i the portion attributable to impurities and imperfections. The phonon contribution ρ_{ph} is temperature dependent; at low temperatures the phonons should be "frozen out": that is, the lattice vibration amplitudes should be very small, so the low temperature resistivity should be approximately equal to

ρ_i . This term in equation (11) is referred to as the residual resistivity, and is temperature independent. This result, along with equation (11), is known as the Matthiessen rule. The ratio of $\rho(5K)/\rho(300K)$ is thus a measure of the relative amount of impurities and imperfections in a given sample relative to other samples of the material: a lower value of $\rho(5K)/\rho(300K)$ indicates fewer impurities and defects.

B. Results and Discussion

In Figures 8 and 9, the resistivity as a function of temperature divided by the resistivity at room temperature is plotted for the materials in this study. The experimental scatter for some samples was caused by their low resistance, which made precise voltage measurements difficult; however, the general shape of the curve was not affected by these uncertainties. The data for ErPd_2Sn was normalized according to data taken in the dilution refrigerator which shows that the material becomes superconducting at 0.7K (see Chapter VI).

Van der Pauw²¹ showed that the resistivity of a flat sample of thickness D with an arbitrarily-shaped perimeter could be calculated by solving the equation

$$\exp\left(-\frac{\pi R_{ab,cd} D}{\rho}\right) + \exp\left(-\frac{\pi R_{bc,da} D}{\rho}\right) = 1 \quad (12)$$

for ρ , given the resistances $R_{ab,cd}$ and $R_{bc,da}$. Wires are attached at four points around the circumference of the sample,

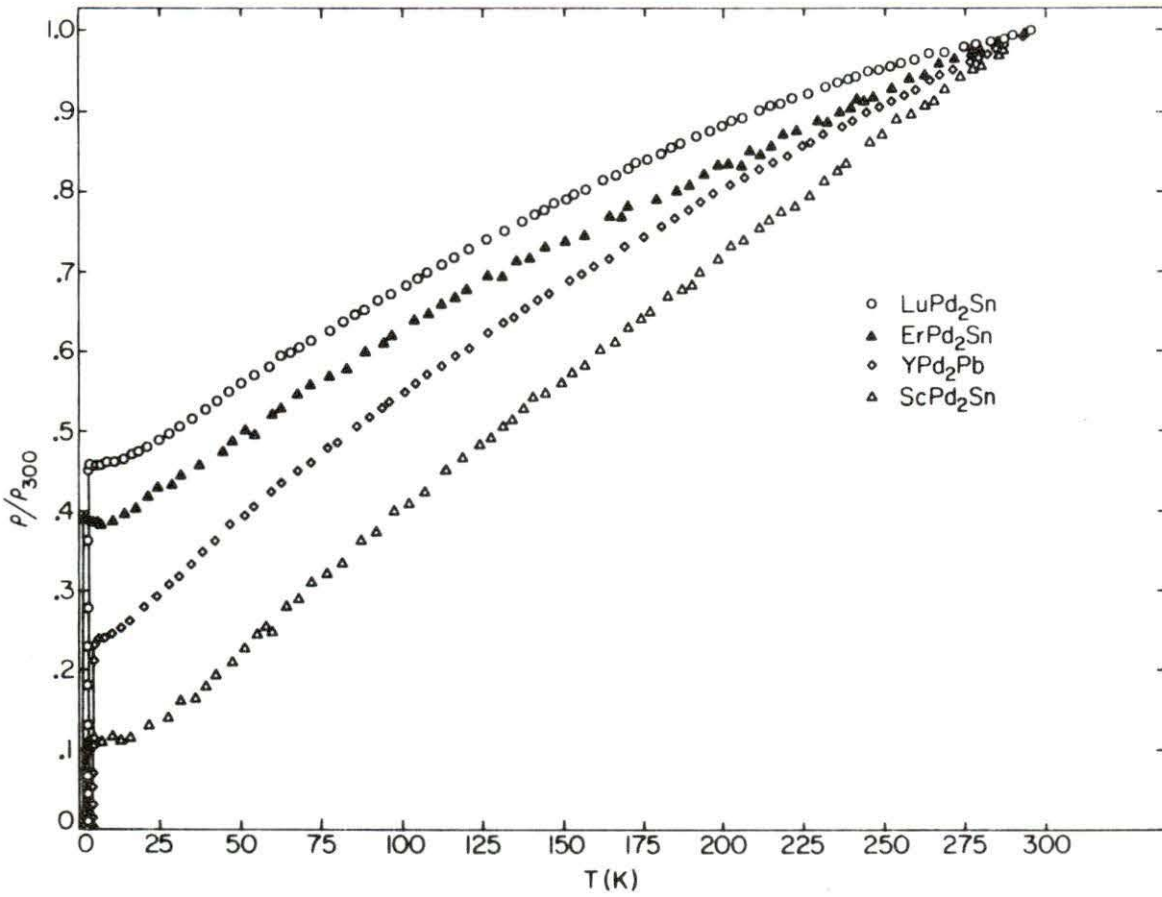


Figure 8. Electrical resistivity versus temperature for some Heusler superconductors

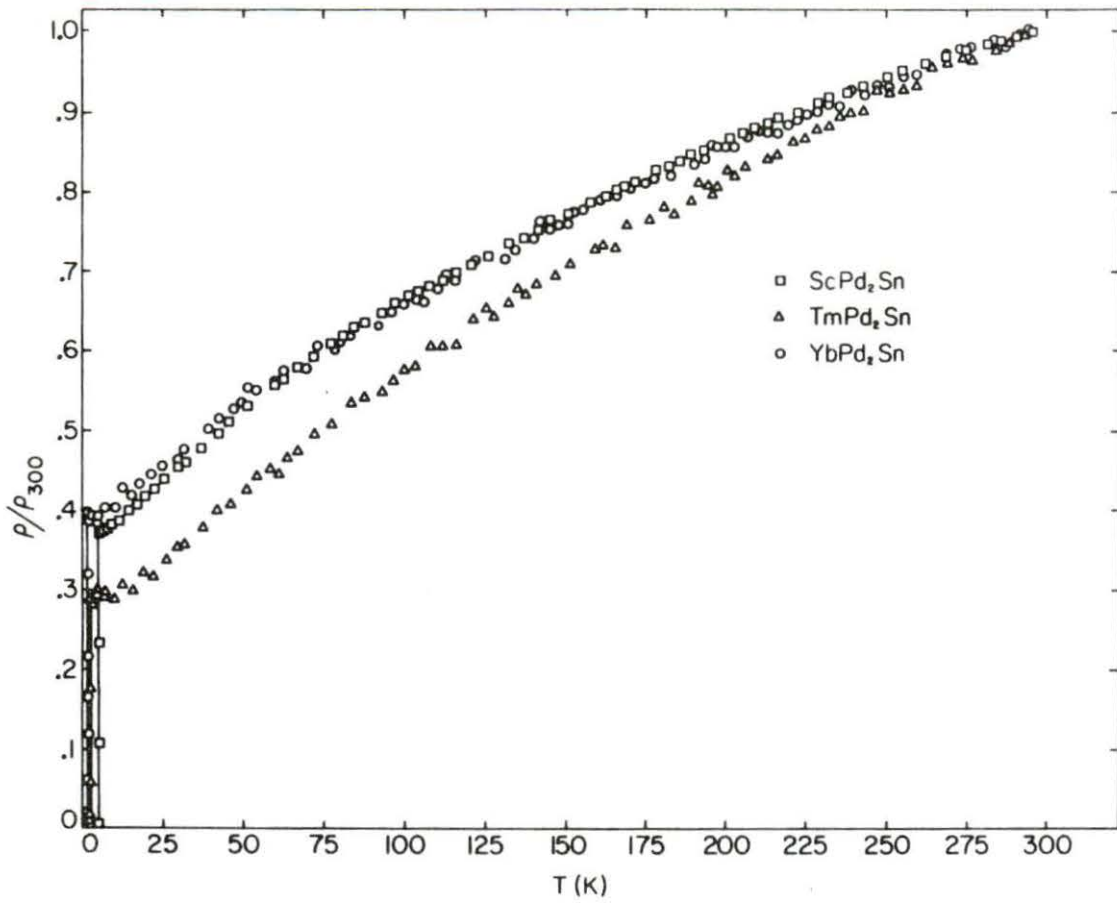


Figure 9. Electrical resistivity versus temperature for some Heusler superconductors

and the contacts are cyclically designated a, b, c, and d. Resistance $R_{ab,cd}$ is defined as the potential difference $V_d - V_c$ between contacts d and c per unit current through contacts a and b; resistance $R_{bc,da}$ is defined similarly. Equation (12) is valid if (i) the contacts are placed in successive positions along the circumference of the sample, (ii) the contacts are sufficiently small (relative to the size of the sample), (iii) the sample is uniform in thickness, and (iv) the sample contains no isolated holes. All these requirements were met by the samples used. Because equation (12) is a non-linear equation, it was solved numerically for the resistivity values.

Table 5 gives the resistivities at room ($\sim 300\text{K}$) and liquid helium ($\sim 5\text{K}$) temperatures and the ratio $\rho(5\text{K})/\rho(300\text{K})$ for the materials in this study; these quantities are also shown in Figure 10. The resistivity values are similar with the exception of the ErPd_2Sn sample, which has resistivities approximately twice as large as the others. This may be due to increased lattice disorder in that sample (since microscopic examination revealed no large-scale inhomogeneities or cracks). The materials have $\rho(5\text{K})/\rho(300\text{K})$ ratios ranging from 0.104 for ScPd_2Sn to 0.459 for LuPd_2Sn .

Table 5. Electrical resistivity values at 300K and 5K

compound	ρ (300K) ($\mu\Omega$ -cm)	ρ (5K) ($\mu\Omega$ -cm)	ρ (5K)/ ρ (300K)
ScPd ₂ Sn	86.38	8.98	0.104
YPd ₂ Sn	70.45	26.07	0.370
YPd ₂ Pb	74.38	17.93	0.241
ErPd ₂ Sn	137.54	52.95	0.385
TmPd ₂ Sn	52.48	14.54	0.277
YbPd ₂ Sn	55.87	21.73	0.389
LuPd ₂ Sn	64.40	29.56	0.459

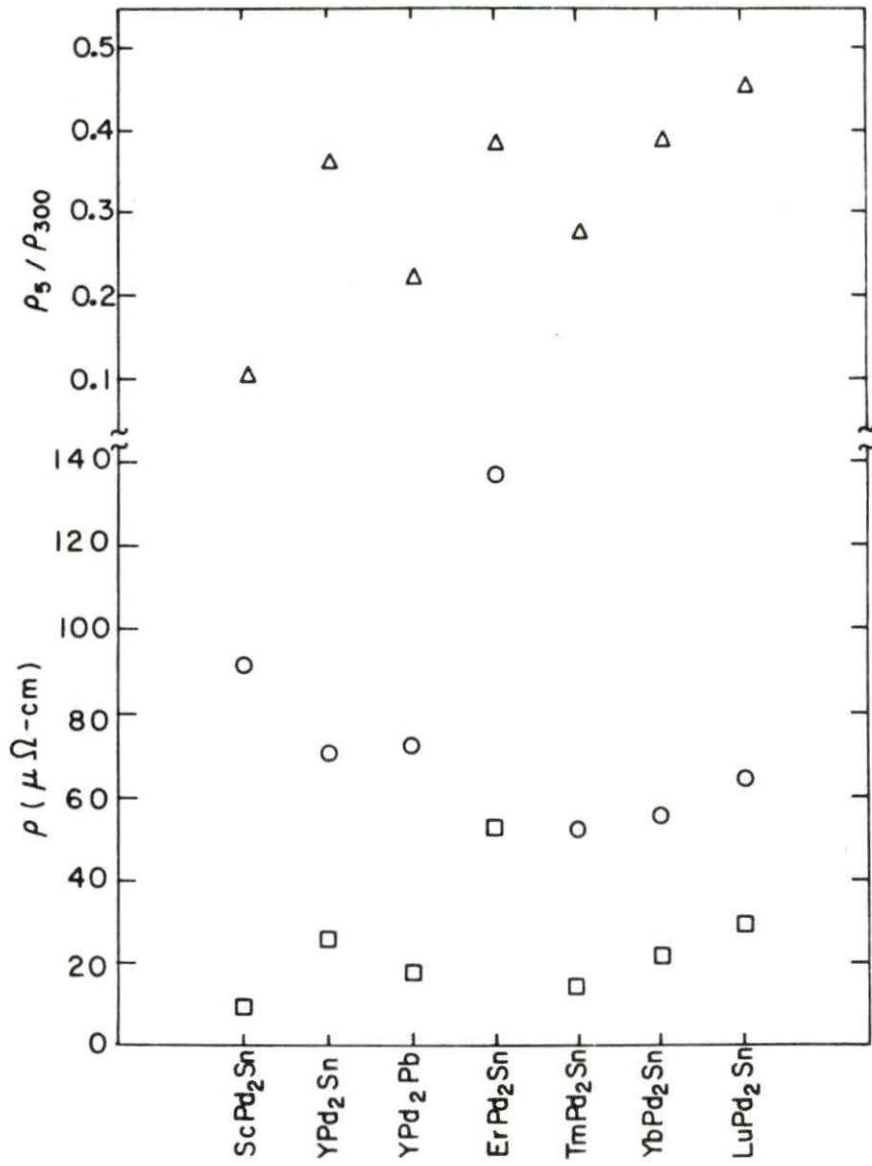


Figure 10. Electrical resistivity at 5 K (\square), 300 K (\circ) and ρ_5/ρ_{300} (Δ) for some Heusler superconductors

VI. ErPd_2Sn

Measurements of the magnetic susceptibility of a bulk sample of ErPd_2Sn were made using the ac susceptibility technique mentioned previously. No impurity peaks were observed in an x-ray diffraction pattern of this sample, indicating if any impurity phases were present, they were below the minimum detectable limit of about 5%. The sample was cooled to 0.060K using a S.H.E. Corporation helium dilution refrigerator, and warmed using a heater mounted just above the sample holder. Data for both cooling and warming are shown in Figures 11 and 12. The susceptibility of a piece of bulk aluminum of approximately the same mass as the sample of ErPd_2Sn was also measured in an adjacent sample holder for comparison.

An increase in the magnetic susceptibility from 10 to 0.8K is possibly indicative of magnetic ordering of the Er atoms, and the sudden decrease in susceptibility (midpoint 0.55K) suggests a superconducting transition. The size and direction of the change in susceptibility of the sample is comparable to that of the aluminum piece, which had a superconducting transition at 1.2K, which one would expect if the bulk of the sample became superconducting. The thermal hysteresis present appears to be inherent in the sample, though it may be partially due to the proximity of the heater to the thermometer.

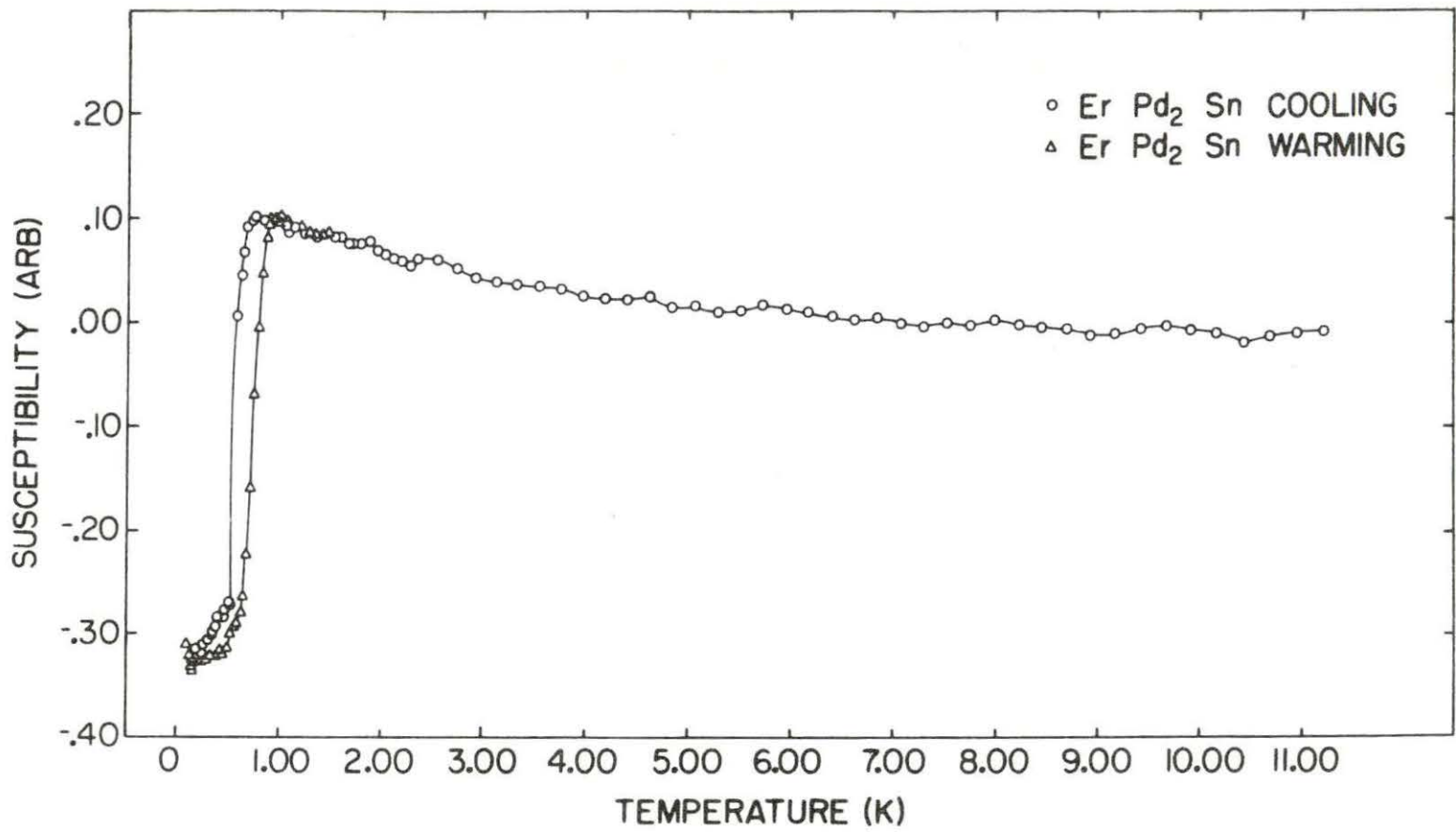


Figure 11. Magnetic susceptibility versus temperature for ErPd₂Sn sample

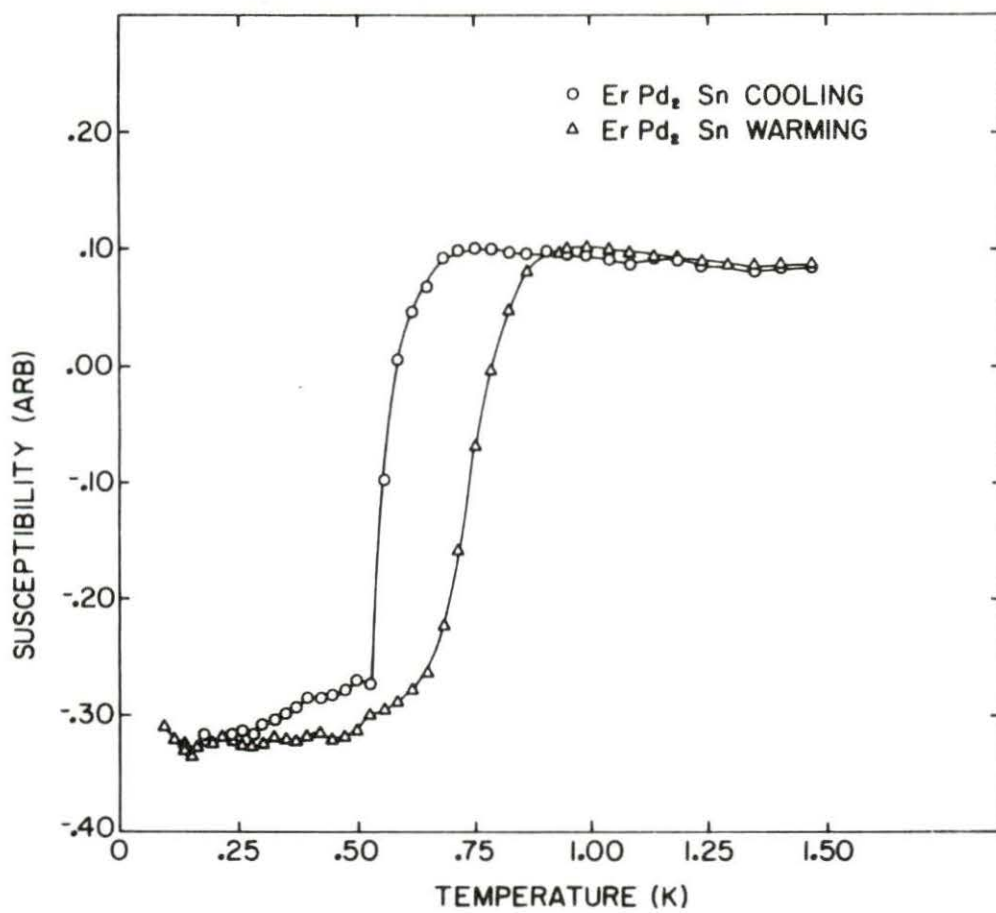


Figure 12. Magnetic susceptibility versus temperature below 1.5 K for ErPd_2Sn sample

Ishikawa et al.¹⁶ reported that ErPd_2Sn had a magnetic transition at 0.7K, and Raub et al.³⁷ determined superconducting transition temperatures for the palladium-tin compounds PdSn , Pd_2Sn , and Pd_3Sn_2 in the range of 0.4 to 0.7K. While it is believed that the sample was single-phased, a possible explanation for the apparent superconducting transition might be a palladium-tin impurity phase present on grain boundaries; the sample may contain regions, some of which may be ordering magnetically, and others which may become superconducting at approximately the same temperature. Several measurements should be made in the future to further investigate this phenomenon. The magnetic susceptibility should be measured using a powdered sample of ErPd_2Sn to decrease the possibility of screening effects by grain-boundary impurities; the heat capacity as a function of temperature should be measured to provide an experimental test for bulk superconductivity.

VII. SUMMARY AND CONCLUSIONS

Annealing of as-cast Heusler superconductors decreases lattice disorder as indicated by increases in the lattice parameter and the superconducting transition temperature. After annealing for two days at 1000°C, the lattice parameter of a sample of LuPd₂Sn saturated at a value of 6.644 Å, an increase of 4mÅ from the as-cast value, while T_c saturated at 2.98K, an increase of 0.19K. Changes of this magnitude seem to be reproducible. The increase in lattice parameter is attributed to insertion of the relatively large Lu atoms into the Pd sublattice, and the increase in T_c is attributed to a decrease in potential fluctuations caused by disorder, sharpening the density of states curve. These results suggest that the transition temperature is a sensitive parameter of the relative crystallographic order in these materials.

The transition temperature of the Heusler superconductors seems to have a simple linear dependence on pressure explained by simple stiffening of the lattice under increasing pressure to 20 kbar. Values of dT_c/dP ranged from -1.449x10⁻⁵ K/bar for ScPd₂Sn to -2.620x10⁻⁵ K/bar for TmPd₂Sn. The sharp structure in the density of states suggested by Ishikawa et al.²⁸ to explain the sensitivity of T_c to tin concentration was not demonstrated at the pressures achieved in this study. The linear relationship between T_c and dT_c/dP noted by Vining and Shelton in the Chevrel phase materials and iron silicides

and suggested by them to be a universal first approximation in such systems seems valid for most of the materials of this study; deviations from this linear behavior are apparently due to magnetic suppression of T_c .

The lack of sudden changes in the resistivity of the samples as a function of temperature would suggest that Heusler materials do not undergo any structural phase transitions in the temperature regime studied, that is, below room temperature. The value of $\rho(5K)/\rho(300K)$ ranged from 0.104 for ScPd_2Sn to 0.459 for LuPd_2Sn . Measurements of the resistivity may be used in the future to estimate lattice disorder in these materials.

Data indicating a superconducting transition in ErPd_2Sn is presented. If superconducting, this material would contain the largest percentage of magnetic atoms (25 atomic % Er) of any known superconductor. The presence of superconducting Pd-Sn impurities on grain boundaries is a possible explanation of the results.

Several measurements should be made in the future to illuminate some of the phenomena in this thesis. A quantitative determination of the effects of disorder on superconducting transition temperature, possibly via resistivity measurements, should be made. This may help us understand the large sample-to-sample variations in T_c of these materials.

Pseudo-ternary systems, like $(\text{Sc},\text{Y})\text{Pd}_2\text{Sn}$, $\text{YPd}_2(\text{Sn},\text{Pb})$, and $(\text{Yb},\text{Lu})\text{Pd}_2\text{Sn}$ may help illustrate the effects of lattice parameter and magnetic atoms on transition temperature. Accurate determination of the Gruneisen parameters (via specific heat measurements) and bulk moduli of some Heusler superconductors will increase the accuracy with which the calculated pressure-dependent quantities like $\langle\omega^2\rangle$, λ , and η are known. Lastly, measurements of the specific heat of ErPd_2Sn will help determine if the apparent superconductivity in the material is a bulk property or due to impurities.

VIII. REFERENCES

1. See, for example, Ternary Superconductors, G. K. Shenoy, B. D. Dunlap, F. Y. Fradin, eds., (North Holland, Amsterdam, 1981) and Superconductivity in Ternary Compounds, Vol. 1 and 2, O. Fischer, M. B. Maple, eds., (Springer-Verlag, Berlin, 1982).
2. R. N. Shelton, in Superconductivity in d- and f-Band Metals 1982, W. Buckel, W. Weber, eds., (Kernforschungszen-
trum, Karlsruhe, 1982), pg. 123.
3. R. Chevrel, M. Sergent, J. Prigent, J. Solid State Chem. 3, 515 (1971).
4. B. T. Matthias, E. Corenzwit, A. S. Cooper, H. E. Barz, Proc. Natl. Acad. Sci. USA 74, 1734 (1977).
5. D. C. Johnston, Solid State Commun. 24, 699 (1977).
6. R. N. Shelton, J. Less Common Metals 62, 191 (1978).
7. H. C. Ku and R. N. Shelton, Mat. Res. Bull. 15, 1441 (1980).
8. R. N. Shelton, B. A. Karcher, D. R. Powell, R. A. Jacobson, H. C. Ku, Mat. Res. Bull. 15, 1445 (1980).
9. H. F. Braun, Phys. Lett. 75A, 386 (1980).
10. C. U. Segre and H. F. Braun, Solid State Commun. 35, 735 (1980).
11. J. P. Remeika, G. P. Espinoza, A. S. Cooper, H. Barz, J. M. Rowell, D. B. McWhan, J. M. Vandenberg, D. E. Moncton, Z. Fisk, L. D. Woolf, H. C. Hamaker, M. B. Maple, G. Shirane, W. Thomlinson, Solid State Commun. 34, 923 (1980).
12. See, for example, P. J. Webster and K. R. A. Ziebeck, J. Phys. Chem. Solids 34, 1647 (1973) and G. R. MacKay, C. Blaauw, J. Judah, W. Leiper, J. Phys. F: Metal Phys. 8, 305 (1978).
13. F. Heusler, Verhandl. Deut. Phys. Ges. 5, 219 (1903).
14. E. Uhl, Ph.D. Thesis, Universitat Wien (1980).
15. E. Uhl, J. Mag. Mag. Materials 25, 121 (1981).

16. M. Ishikawa, J-L. Jorda, A. Junod, in Superconductivity in d- and f-Band Metals 1982, W. Buckel, W. Weber, eds., (Kernforschungszentrum, Karlsruhe, 1982), pg. 141.

17. P. R. Bevington, Data Reduction and Error Analysis for the Physical Sciences, (McGraw-Hill, New York, 1969), pg. 104.

18. K. Yvon, W. Jeitschko, E. Parthé, J. Appl. Cryst. 10, 73 (1977).

19. T. F. Smith, J. Low Temp. Physics 6, 171 (1972).

20. A. Eiling and J. S. Schilling, J. Phys. F: Metal Phys. 11, 623 (1981).

21. L. J. van der Pauw, Philips Research Reports 13, 1 (1958).

22. D. E. Cox, A. R. Sweedler, S. Moehlecke, L. R. Newkirk, F. A. Valencia, in Superconductivity in d- and f-Band Metals, H. Suhl, M. B. Maple, eds., (Academic Press, New York, 1980), pg. 335.

23. M. Lehman, C. Nolscher, H. Adrian, J. Bieger, L. Soldner, G. Saemann-Ischenko, in Superconductivity in d- and f-Band Metals 1982, W. Buckel, W. Weber, eds., (Kernforschungszentrum, Karlsruhe, 1982), pg. 107.

24. R. Dynes, J. Rowell, P. Schmidt, in Ternary Superconductors, G. Shenoy, B. Dunlap, F. Fradin, eds., (North Holland, Amsterdam, 1982), pg. 169.

25. H. Adrian, F. Pfirsch, R. Behrle, G. Saemann-Ischenko, in Superconductivity in d- and f-Band Metals 1982, W. Buckel, W. Weber, eds., (Kernforschungszentrum, Karlsruhe, 1982), pg. 107.

26. A. Eiling, J. S. Schilling, H. Bach, in Physics of Solids Under High Pressure, J. S. Schilling, R. N. Shelton, eds., (North Holland, Amsterdam, 1981), pg. 385.

27. R. I. Boughton, J. L. Olsen, C. Palmy, Progress in Low Temperature Physics, Vol. 16, C. J. Gorter, ed., (North Holland, Amsterdam, 1970), pg. 163.

28. T. F. Smith, Superconductivity in d- and f-Band Metals, D. H. Douglass, ed., (AIP, New York, 1972), pg. 293.

29. R. N. Shelton and R. P. Dougherty, *Physica* 107B, 475 (1981).
30. C. U. Segre and H. F. Braun, in *Physics of Solids Under High Pressure*, J. S. Schilling, R. N. Shelton, eds., (North Holland, Amsterdam, 1981), p. 381.
31. C. B. Vining and R. N. Shelton, 9th AIRAPT International High Pressure Conference, July 25, 1983, (North Holland, to be published).
32. R. J. Higgins and H. D. Haehn, *Phys. Rev.* 182, 649 (1969) and V. G. Bar Yakhtar, V. V. Gann, V. I. Makarov, T. A. Ignateva, *Sov. Phys. JETP* 35, 591 (1972).
33. W. L. McMillan, *Phys. Rev.* 167, 331 (1968).
34. J. W. Garland and K. H. Benneman, in *Superconductivity in d- and f-Band Metals*, D. H. Douglass, ed., (AIP, New York, 1972), p. 255.
35. T. H. K. Barron, J. C. Collins, C. White, *Advances in Physics* 29, 609 (1980).
36. J. Kübler, *J. Phys. F: Metal Phys.* 8, 2301 (1978).
37. C. J. Raub, W. H. Zachariasen, T. H. Geballe, B. T. Matthias, *J. Phys. Chem. Solids* 24, 1093 (1963).

IX. ACKNOWLEDGEMENTS

I would like to thank all those who aided me during my graduate work at Iowa State University. I deeply appreciate the help and concern of the faculty, staff, secretaries, technicians, and fellow graduate students in the Physics Department who made my time in Ames exciting and valuable.

Admiration, as well as gratitude, is felt for Dr. Robert N. Shelton, who advised me and helped in the production of this work even though he was half the world away. I am indebted to Dr. Cronin B. Vining for his advice and encouragement. I appreciate the help and counsel of my graduate committee: Dr. Douglas K. Finnemore, Dr. John R. Clem, and Dr. Karl Gschneidner, Jr. Without the patience and humor of Mr. Peter Klavins, much of this work would not have been possible. I owe many thanks to Pat Thiede, who patiently typed this thesis.

Most importantly, this work is dedicated to my fiancée Jan, whose patience and caring have made it all worthwhile.

X. APPENDIX: SOURCES AND PURITIES OF
STARTING MATERIALS

element	source	purity ^a	
Sn	Indium Corp. of America	99.999+% (weight), powder	
Pb	Materials Research Corp.	lot 82/2282, rod	
		major impurities:	C 121 ppm O 65 ppm Sn 3.5 ppm Fe 3.7 ppm
		other impurities all	<3 ppm
Pb	from Government Stockpile, refined by Alfa Chemicals	99.8% (weight), powder	
Sc	Ames Laboratory	batch 112481, ingot	
		major impurities:	H 490 ppm O 188 ppm W 84 ppm C 83 ppm Fe 53 ppm Lu 50 ppm F 28 ppm Ta 7.3 ppm N 6.4 ppm La 5 ppm Ce 4.2 ppm
		other impurities all	<4 ppm
Y	Ames Laboratory	batch 2276, ingot	
		major impurities:	O 240 ppm Fe 46 ppm H 14 ppm C 11.5 ppm N 10.3 ppm

			Cl	9	ppm
			W	7	ppm
			Cu	6.4	ppm
			Ce	4	ppm
			Gd	4	ppm
		other impurities all		<4	ppm
Er	Ames Laboratory	batch 71177, ingot			
		major impurities:	Ta	30	ppm
			O	30	ppm
			C	10	ppm
			Fe	6.6	ppm
			H	6	ppm
		other impurities all		<4	ppm
Tm	Ames Laboratory	batch 32878, ingot			
		major impurities:	Fe	35	ppm
			C	24	ppm
			F	14	ppm
			Cu	11	ppm
			Cl	10	ppm
			Ce	8	ppm
		other impurities all		<4	ppm
Yb	Ames Laboratory	batch 62973, ingot			
		major impurities:	O	38	ppm
			Fe	30	ppm
			Ca	<10	ppm
			C	10	ppm
			H	8	ppm
			Lu	7	ppm
			La	6	ppm
			Gd	6	ppm
		other impurities all		<4	ppm

element	source	purity ^a	
Lu	Ames Laboratory	batch 51177, ingot	
		major impurities:	O 33 ppm
			W 31 ppm
			Cu 20 ppm
			La 11 ppm
			Ni 10 ppm
			Fe 6.1 ppm
			H 5 ppm
		other impurities all	<4 ppm

^aAll purities are in atomic ppm unless otherwise noted.